



# Microgliosis and neuronal proteinopathy in brain persist beyond viral clearance in SARS-CoV-2 hamster model

Christopher Käufer,<sup>a</sup> Cara S. Schreiber,<sup>a,e</sup> Anna-Sophia Hartke,<sup>a,e</sup> Ivo Denden,<sup>a</sup> Stephanie Stanelle-Bertram,<sup>b</sup> Sebastian Beck,<sup>b</sup> Nancy Mounogou Kouassi,<sup>b</sup> Georg Beythien,<sup>d</sup> Kathrin Becker,<sup>d</sup> Tom Schreiner,<sup>d</sup> Berfin Schaumburg,<sup>b</sup> Andreas Beineke,<sup>d,e</sup> Wolfgang Baumgärtner,<sup>d,e</sup> Gülsah Gabriel,<sup>b,c</sup> and Franziska Richter<sup>a,e,\*</sup>

<sup>a</sup>Department of Pharmacology, Toxicology and Pharmacy, University of Veterinary Medicine Hannover, 30559 Hannover, Germany

<sup>b</sup>Leibniz Institute for Experimental Virology, Hamburg, Germany

<sup>c</sup>Institute for Virology, University for Veterinary Medicine Hannover, 30559 Hannover, Germany

<sup>d</sup>Department of Pathology, University of Veterinary Medicine Hannover, 30559 Hannover, Germany

<sup>e</sup>Center for Systems Neuroscience, Hannover, Germany

## Summary

**Background** Neurological symptoms such as cognitive decline and depression contribute substantially to post-COVID-19 syndrome, defined as lasting symptoms several weeks after initial SARS-CoV-2 infection. The pathogenesis is still elusive, which hampers appropriate treatment. Neuroinflammatory responses and neurodegenerative processes may occur in absence of overt neuroinvasion.

**Methods** Here we determined whether intranasal SARS-CoV-2 infection in male and female syrian golden hamsters results in persistent brain pathology. Brains 3 (symptomatic) or 14 days (viral clearance) post infection versus mock (n = 10 each) were immunohistochemically analyzed for viral protein, neuroinflammatory response and accumulation of tau, hyperphosphorylated tau and alpha-synuclein protein.

**Findings** Viral protein in the nasal cavity led to pronounced microglia activation in the olfactory bulb beyond viral clearance. Cortical but not hippocampal neurons accumulated hyperphosphorylated tau and alpha-synuclein, in the absence of overt inflammation and neurodegeneration. Importantly, not all brain regions were affected, which is in line with selective vulnerability.

**Interpretation** Thus, despite the absence of virus in brain, neurons develop signatures of proteinopathies that may contribute to progressive neuronal dysfunction. Further in depth analysis of this important mechanism is required.

**Funding** Federal Ministry of Health (BMG; ZMV I 1-2520COR501), Federal Ministry of Education and Research (BMBF 01KI1723G), Ministry of Science and Culture of Lower Saxony in Germany (14 - 76103-184 CORONA-15/20), German Research Foundation (DFG; 398066876/GRK 2485/1), Luxemburgish National Research Fund (FNR, Project Reference: 15686728, EU SCi-PHE-CORONAVIRUS-2020 MANCO, no > 101003651).

**Copyright** © 2022 The Author(s). Published by Elsevier B.V. This is an open access article under the CC BY-NC-ND license (<http://creativecommons.org/licenses/by-nc-nd/4.0/>)

**Keywords:** Alpha-synuclein; Tau; Neuroinfection; Neurodegenerative disease; Animal model

**Abbreviations:** PD, Parkinson's Disease;  $\alpha$ -syn,  $\alpha$ -synuclein

\*Corresponding Author: Franziska Richter DVM, Ph.D., Department of Pharmacology, Toxicology and Pharmacy, University of Veterinary Medicine Hannover, Foundation, Bünteweg 17, 30559 Hannover, Germany

E-mail address: [franziska.richter@tiho-hannover.de](mailto:franziska.richter@tiho-hannover.de) (F. Richter).

## Introduction

Neurological symptoms are common during acute COVID-19 (up to 67% of patients), may persist after elimination of SARS-CoV-2 or even emerge de novo weeks after disease remission.<sup>1-5</sup> Neurologic, neuropsychological and neuropsychiatric symptoms such as cognitive disturbances, sleep disturbances, headache, dizziness, depression, anxiety, gait disorder and general fatigue frequently occur in post-COVID-19 syndrome, a

### Research in context

#### *Evidence before this study*

Estimations of post-COVID-19 syndrome prevalence range from 10-85%, depending on disease severity and other factors. Asymptomatic or mild SARS-CoV-2 infections are also frequently associated with long lasting neurological symptoms, such as headache, fatigue, and cognitive disturbance. Imaging studies and biomarker assessments in patients point to ongoing neuroinflammatory and degenerative processes. The underlying mechanisms are largely unknown, which hampers the application of rational disease-modifying therapeutics.

#### *Added value of this study*

We performed immunohistochemical studies on brains of the well-established SARS-CoV-2 hamster model and observed increase in markers of neuroinflammation and accumulation of proteins implicated in the pathogenesis of neurodegenerative diseases. Importantly, this observation was at a time point of apparently full recovery from infection and in absence of overt viral protein in brain.

#### *Implications of all the available evidence*

Together with findings in post-COVID-19 patients our results implicate that the potential presence of neurodegenerative processes requires urgent attention and further studies to guide appropriate diagnostics and therapeutic intervention.

highly debilitating condition developed four or more weeks after SARS-CoV-2 infection.<sup>6,7</sup> The pathogenesis of these symptoms is still elusive, and there is currently no effective treatment apart from extensive rehabilitation plans.<sup>8</sup> The diversity of symptoms clearly indicates involvement of many brain regions, and cannot be explained by isolated thromboembolic events. It is still debated whether and how SARS-CoV-2 enters the brain. Some studies suggest the olfactory mucosa or local alterations of the blood brain barrier as entry points, but across available studies it appears that such events are localized, specific to receptive cells and do likely not lead to widespread viral replication in the brain, even in severe COVID-19.<sup>9-12</sup> Neuropathological and molecular findings of patients that died with COVID-19 encompass microglia activation, neuronophagia, but also haemorrhagic infarcts among other observations, while levels of detectable virus appeared low.<sup>13-20</sup> The severity of COVID-19 in these patients, driven for example by overt systemic inflammation, may have contributed to brain pathology. Thus, authors recently concluded that further studies are needed to define whether these pathologies, if present in patients who survive COVID-19, might contribute to chronic neurological

problems.<sup>21</sup> In fact, the development of neurological symptoms as described for several months to years after mild or asymptomatic SARS-CoV-2 infection are unlikely to involve severe encephalitis or overt widespread neurodegeneration. Instead, local blood-brain-barrier leakage due to virus invasion in some perivascular compartments or via the olfactory bulb may be sufficient to initiate a process of dysregulation of cellular homeostasis, local astrogliosis and axonal damage.<sup>9,22-25</sup> Such persistence of neurological symptoms, up to now at least one year in a majority of patients,<sup>6,7,26,27</sup> and also including young adults with mild COVID-19,<sup>28</sup> points towards tenacity or even progression of these processes. The potential mechanisms that drive disease progression in the brain beyond viral clearance represent a critical knowledge gap towards application of effective therapy. In progressive neurodegenerative diseases, alpha-synuclein and tau are upregulated as part of the neuronal stress response, leading to intracellular accumulation, post-translational modification/truncation, loss or gain of toxic function, and perpetuating toxicity to the neuron. These processes are hallmarks of synucleinopathies (e.g. Parkinson's disease) or tauopathies (e.g. Alzheimer's disease, progressive supranuclear palsy).<sup>29-32</sup> In fact, neurodegenerative disorders display protein pathology in the olfactory bulb, typically associated with deficits in olfactory perception in the very early phase of these diseases.<sup>33</sup> Such pathology can spread prion-like across neurons, or even from the gut nervous system to the brain.<sup>34-36</sup> Therefore, even subtle local alterations can present a starting point to more widespread progressive pathology. Here we present evidence that upon intranasal inoculation of SARS-CoV-2 in hamsters, neurodegenerative processes are initiated from microglia activation in the olfactory bulb to accumulation of hyper-phosphorylated tau and alpha-synuclein protein in cortical neurons.

## Methods

### SARS-CoV-2 infection of hamsters

All animal experiments were performed under BSL-3 conditions as described previously.<sup>37</sup> Male and female Syrian Golden Hamsters of ages 8-10 weeks were intranasally infected with 10<sup>5</sup> plaque forming units (p.f.u.) of SARS-CoV-2<sup>37</sup> dissolved in 50 µl of PBS under ketamine xylazine anaesthesia (150 mg/kg & 10 mg/kg). Mock infected animals intranasally received 50 µl of PBS. Following infection, the hamsters were clinically evaluated daily and sacrificed on days 3 (high virus titers in periphery and onset of clinical disease) or 14 post infection (animals recovered from infection and no virus is detectable in animals) by injection of a high dose of pentobarbital. Per group 10 animals were used, amounting to 40 animals in total. Groups were treated in parallel to minimize confounding factors. One animal did not

survive until day 14 post infection and was hence excluded from this group.

### Ethics

All animal experiments were carried out in strict accordance with the guidelines of German animal protection law and were approved by the Behörde für Gesundheit und Verbraucherschutz, State of Hamburg, Germany (NO32/2020).

### Tissue processing and histological evaluation

Succeeding euthanasia, brains were harvested and placed in 10% formalin for fixation and inactivation of SARS-CoV-2 in the tissue. Noses were cut from the skull and also placed in formalin for inactivation. Following inactivation and fixation, brain tissue was trimmed, embedded in paraffin and FFPE-slides were produced. Noses were incubated in EDTA solution to decalcify bone tissue prior to embedding and sectioning.<sup>38,39</sup> Three  $\mu\text{m}$  sections were stained with hematoxylin and eosin (HE) for histopathological examination by light microscopy as previously described.<sup>38,39</sup>

### Immunohistochemistry

For immunohistochemical analysis FFPE-sections were treated as previously published (Käufer et al. 2018,<sup>40</sup> Becker et al. 2021<sup>38</sup>). Briefly, tissue sections were deparaffinized, rehydrated and then demasked by boiling the slides in citric acid buffer. Afterwards, sections were blocked using a goat serum solution and then incubated with primary antibody solution over night at 4°C (primary antibodies used can be found in supplementary Tab.1). On the following day, sections were incubated in secondary antibody solution (cf. supplementary Table 1) and cover slipped using ProLong™ Gold Antifade Mountant with DAPI (Thermo Fisher). Stained sections were digitized using a Zeiss Axio Observer 7 microscope using either 10x or 20x magnification lenses and a Zeiss Colibri 7 LED light source. The software used for scanning was MBF Stereo Investigator 11. Scanned images were further analyzed using the Fiji package of Image J<sup>41</sup> Regions that were analyzed are schematically illustrated in Figure 1 a, l, n and Figure 2 a, i: The nasal turbinates, the olfactory bulb, the piriform cortex, the suprahypocampal cortex and the hippocampus, as well as the hilus region of the dentate gyrus. The number of evaluated slides per tissue area varies depending on the availability of the tissue per slide. Also, due to BSL3 conditions, the tissue was not perfused by transcardial perfusion. This results in the presence of residual blood in vessels with blood cells unspecifically stained by fluorescent secondary antibodies, which was indicated in the figures but did not interfere with quantification of assessed marker proteins. All histological analyses were performed in a blinded and randomized fashion and

scientists evaluating brain slides were not aware about the status of infection. The following paragraph provides more details for each staining and quantification procedure: 3 a.) For evaluation of virus positivity, nasal tissue and olfactory bulb were stained for the SARS-CoV-2 Spike S2 protein. Semiquantitative scoring was used to classify tissues into four scores: no virus, low virus, medium virus, high virus (Figure 1 a-c). 3 b.) Ibar-positive cells in the nasal tissue: Ibar1 was stained to evaluate the degree of myeloid cell infiltration/activation in the nasal turbinate tissue as well as the olfactory bulb. Ibar1-positive cells in the nasal tissue were not quantified but are qualitatively displayed to demonstrate the high degree of inflammation following SARS-CoV-2 infection in this tissue. Olfactory bulb Ibar1-positive cells, i.e. microglia, were counted in representative ROIs of nasal slides from both 3 and 14 dpi specimen if sections contained the olfactory bulb. 3 c.) Ibar1-positive cells were further analyzed at both 3 and 14 days post infection in the piriform cortex, the suprahypocampal cortex and the dorsal hippocampus by counting manually. 3 d.) For hyperphosphorylated Tau (p-Tau), the dorsal hippocampus and suprahypocampal cortex were stained with p-Tau primary antibody (phosphorylated at Ser202 and Thr205) and positive cells were counted. Our observations revealed two populations of p-Tau-positive cells: cells with average staining and cells that were very highly stained (i.e. accumulating high amounts of p-Tau protein). We recounted cells by dividing the cell population into two based on intensity threshold. This threshold was set by measuring representative cells of both populations. Cells with intensity above 350 arbitrary intensity units were classified highly-positive for p-Tau. 3 e.) NeuN-positive cells were co-labeled for Tau to evaluate density of neurons that accumulate tau protein. Densities of these cells are high and appeared homogeneous in the examined brain regions, therefore randomly placed rectangular ROIs were analyzed for cell counts. NeuN-positive cells and Tau-positive cells were quantified at the same session and the ratio between double-positive and NeuN-positive cells was calculated. 3 f.) Cells positive for alpha-synuclein (a-syn) were counted as described for tau protein.

### Statistics

A priori sample size determination and power analysis was performed with primary outcome measure number of immune-reactive neurons in cortex. Animals were assigned systematically to treatment groups. All quantifications and analyses were done by investigators blinded to treatment conditions. A priori normality testing (Shapiro-Wilk) was followed by Student's t-tests and Mann Whitney U-tests to compare immunoreactivity in mock versus SARS-CoV-2 infected hamsters. Results from both tests were reported for transparency in figure legends, together with single animal representations.

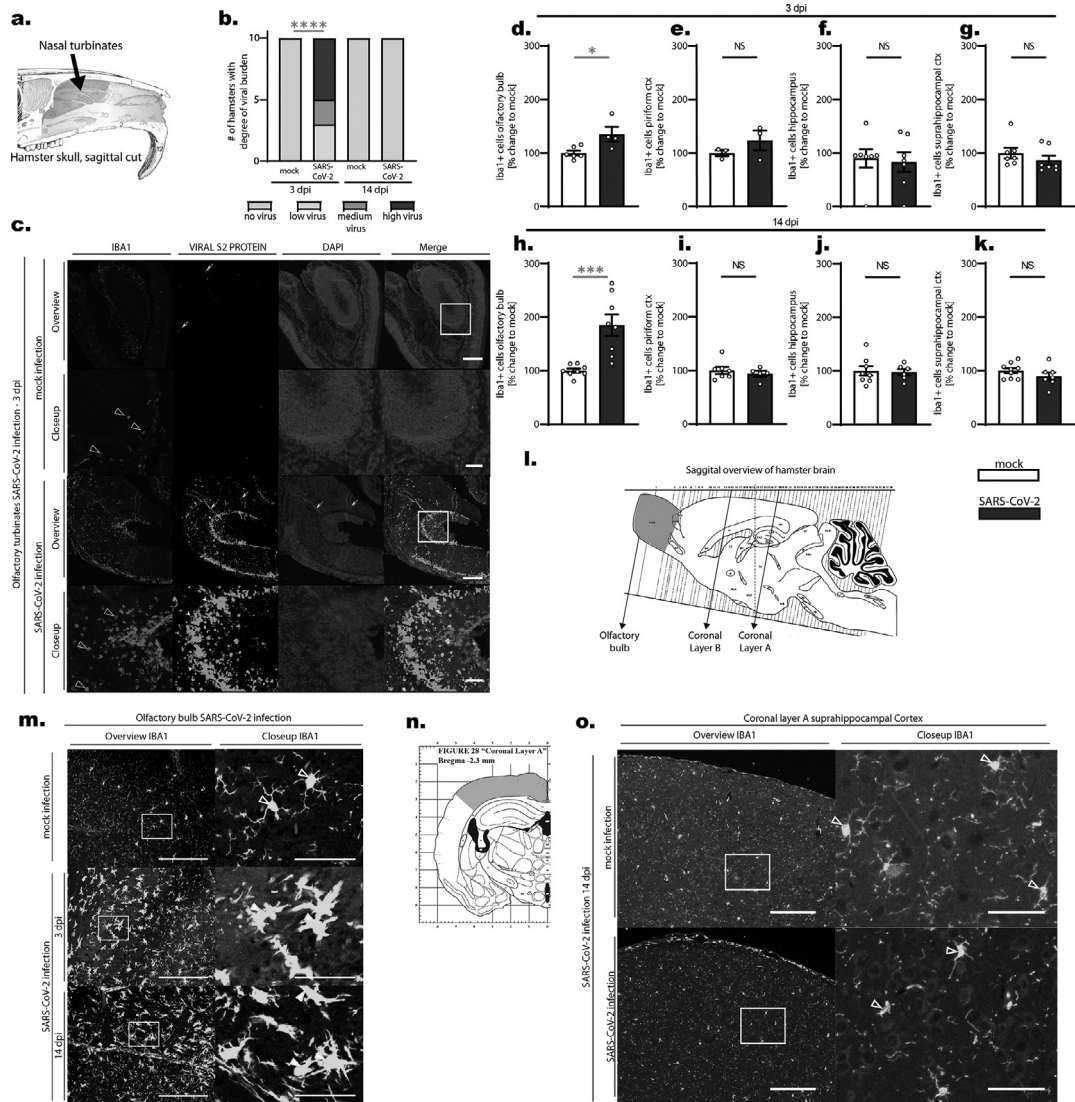


**Figure 1.** a. Schematic depicting a sagittal-cut hamster skull and the position of nasal turbinates evaluated in this study (blue area). b. Viral S2 protein was stained in olfactory turbinates of hamsters following SARS-CoV-2 or mock infection and infection burden was semiquantitatively scored (no virus, low, medium and high degree of virus). Viral protein could only be stained in infected animals 3 days post infection (compare also Figure 1 c). Statistics: infected vs. mock testing animals with viral antigen vs. no antigen present:  $p < 0.0001$  (fisher's test). Data shown represents the number of hamsters with the respective score. c. Immunofluorescent images from nasal tissue stained against IBA1 (myeloid cells), viral S2 protein and DAPI (cell nuclei) from 3 days post infection (mock and SARS-CoV-2 infection). Note the high number of Iba1-positive cells in infected noses compared to the low number of Iba1-positive myeloid cells in the mock infected tissue (hollow arrowheads in Iba-1 (red) images). Also a vast amount of viral S2 protein in different parts of the nasal tissue can be observed (white arrow heads in viral S2 protein (green) images). Artefacts are due to unspecific fluorescence (white arrows). d-k. Statistical evaluation of Iba1-positive cells in different brain regions on 3 dpi (d-g.) and 14 dpi (h-k.). Changes in the number of Iba1-positive cells in 4 different brain regions (d+h. olfactory bulb, e+i. piriform cortex, f+j. hippocampus and g+k. suprahippocampal cortex) are shown as % changes in relation to the mean of mock. Data shown are Box-Plots with mean +/- SEM. Dots represent the individual data values (N). Statistics: mock vs. SARS-CoV-2 infection. \* =  $p < 0.05$ , \*\*\* =  $p < 0.001$  (Mann-Whitney U-test (MWU) and unpaired t-test (t-test)). l. Schematic illustration of the sagittally cut hamster brain, from brain atlas (Morris and Wood, 2001) depicting the evaluated brain regions of the study: Olfactory bulb (violet color, sagittal evaluation), and Coronal Layers A and B. m. Iba1-positive cells (i.e. microglia) in the olfactory bulb from mock and SARS-CoV-2 infected hamsters. While cells from mock infected animals appear to be resting, i.e. they have small cell bodies and fine protrusions (hollow arrowheads), cells from SARS-CoV-2 infected animals appear activated (white arrowheads), i.e. they have enlarged cell bodies and processes, on both 3 and 14 dpi. n. Schematic representation of the suprahippocampal region evaluated. o. Iba1-positive cells in the

Frequencies were compared with Fisher exact test. The significance level was set at  $p < 0.05$  for all analyses. Grubbs test was used to determine outliers ( $p < 0.05$ ). All statistics were calculated using GraphPad Prism (GraphPad Software, Inc., San Diego, CA, USA, 2003) and SigmaPlot 12.0 (Systat Software, Inc., San Jose, CA).

### Role of funders

The funders did not have any role in study design, data collection, data analyses, interpretation or writing of the report.

## Results

### Persisting microgliosis in the olfactory bulb upon SARS-CoV-2 infection

COVID-19 can be induced in hamsters because virus can enter cells via the human-homolog angiotensin-converting enzyme 2 (ACE2).<sup>42</sup> In the past year, the hamster model of SARS-CoV-2 infection has been extensively used to study pathology in various organ systems and to develop novel treatments and vaccines.<sup>38,43-46</sup> This model is currently regarded as close to the human disease process. However, the impact of SARS-CoV-2 infection on the central nervous system is still poorly understood. In order to study effects of SARS-CoV-2 infection in the brain of hamsters we started screening the brains and noses of infected hamsters for the presence of SARS-CoV-2 antigen at an early time point post infection (3 days post infection [dpi]). At 3 dpi hamsters present with weight loss, ragged fur, reduced activity and increased rate of breathing.<sup>43-45,46</sup> In addition, hamsters show a decreased sense of smell supporting decreased function of the olfactory system.<sup>47-49</sup> Histopathological evaluation of the nasal cavity showed large accumulation of mucopurulent exudate in the nasal lumen ( $n = 9$  animals) as well as necrosis ( $n = 9$  animals) and severe infiltration of the olfactory and respiratory mucosa by heterophils and histiocytes ( $n = 10$  animals). While the nasal turbinates of infected hamsters contained massive amounts of viral protein-positive cells (Figure 1 a-c), neither the olfactory bulb, nor the cerebral tissue of infected hamsters contained viral protein (immunohistochemistry data and staining not shown). In another batch of animals, we were able to isolate viral particles from brain homogenate on day 3 post infection. By day 6 post infection, no viral particles could be identified by plaque assay

(data not shown, animals were infected in the same manner as this group of animals). In order to ensure that the persisting presence of viral protein in the nasal mucosa (Figure 1 b-c) and brain tissue did not impact brain tissue homogeneity, we quantified microglia, the resident immune cells of the brain, at 3 dpi in virus versus mock-infected hamsters (Figure 1 d-g, l, m). Although the tissue of the cerebrum, cerebellum and brainstem did not show overt histopathological signs of inflammation, we could observe an increased number of microglial cells (i.e. microgliosis) in the olfactory bulb, the brain region directly adherent to the olfactory tract (i.e. Iba1-positive cells, 34.7 % increase,  $p = 0.0229$  unpaired t-test; Figure 1 d). Strikingly, microgliosis in the olfactory bulb persisted beyond viral clearance from the nasal cavity at 14 dpi (85 % increase,  $p = 0.0009$  unpaired t-test, Figure 1 h), when the nasal mucosa itself showed no ( $n = 1$  animal) or only few to moderate numbers of infiltrating immune cells ( $n = 9$  animals). This points towards an ongoing and potentially progressive neuroinflammatory process in animals that have apparently recovered from the clinical disease. As microglial densities did not differ in the piriform cortex (Figure 1 e-i), the hippocampus (Figure 1 f-j) and the suprahypocampal cortex at 3 or 14 dpi (Figure 1 g+k, n, o) (all  $p > 0.05$  unpaired t-test, Figure 1), this microgliosis appears to be a local proximity-guided response to the intranasal infection and inflammation, which is observable by the massive infiltration of Iba1-positive myeloid cells into the nasal turbinates (Figure 1 c, qualitative analysis).

### Hyper-phosphorylated-tau and alpha-synuclein protein accumulate in cortical neurons beyond viral clearance

Given that brain regions are interconnected, such overt and persisting local neuroinflammation may still result in distinct pathogenic processes in distant but vulnerable neurons.<sup>33,36,50</sup> To further investigate the long term effects of SARS-CoV-2 infection, we therefore analyzed hippocampus and suprahypocampal cortex from animals at recovery post infection (14 dpi) for markers of neurodegenerative processes versus mock controls. Specifically, based on previous experience in slowly progressing neurodegenerative diseases,<sup>29-32</sup> we hypothesized that neuronal homeostasis may be altered observable in accumulation of pathogenic proteins and their potentially more toxic post-translational modifications. To test this hypothesis we quantified total tau protein and hyper-phosphorylated tau as well as total alpha-

suprahypocampal Cortex 14 dpi. No overt differences of microglial cells (hollow arrowheads) could be observed between mock and SARS-CoV-2 infected hamsters. Scale bars: Overview images 200  $\mu\text{m}$ , Closeup images 50  $\mu\text{m}$ .

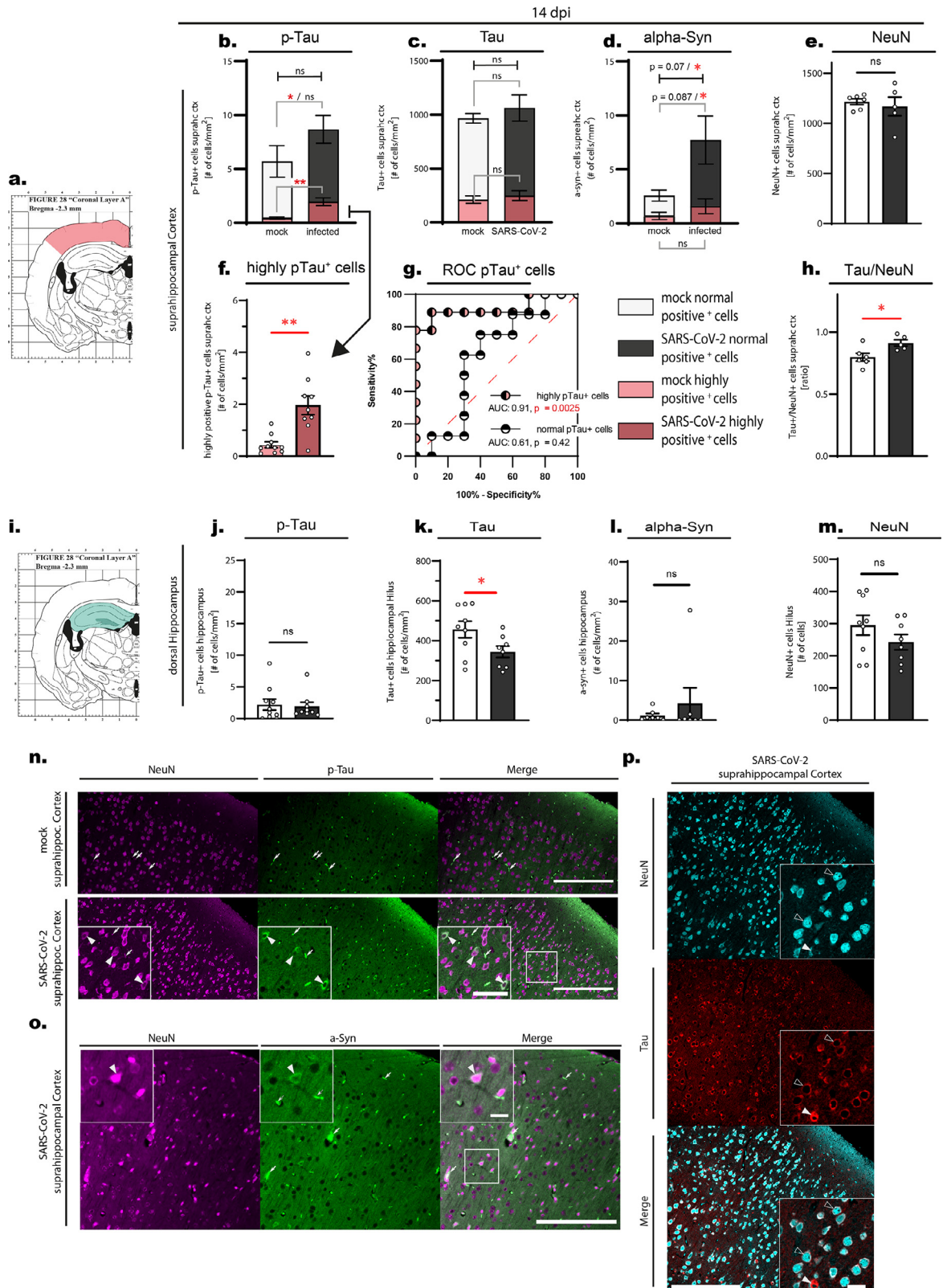


**Figure 2.** All data shown is from animals at the time point 14 days post infection. **a-h.** Evaluation of suprahippocampal p-Tau-positive, Tau-positive, alpha-synuclein-positive and NeuN-positive cells. **a.** Schematic drawing of the approximate position of the

synuclein in neurons (Figure 2). We found a significant increase in the number of cortical neurons with high burden of hyper-phosphorylated tau (Figure 2 a, b, f, n median 0.3314 vs 1.779,  $p = 0.0015$  Mann-Whitney U-test) and an increased alpha-synuclein burden (Figure 2 d, o median 1.690 vs. 7.738 cells/mm<sup>2</sup>,  $p = 0.0279$  one-sided t-test), pointing towards early pathogenic processes also found in proteinopathies. Numbers of highly p-Tau-positive cells are able to reliably differentiate between infected and mock animal (Figure 2 g, AUC 0.91,  $p = 0.0025$ ). In addition, the fraction of total Tau-positive to NeuN-positive cells in the cortex increased in SARS-CoV-2 infected hamsters at 14 dpi (Figure 2 h, median 0.7869 vs. 0.8969,  $p = 0.03$  Mann-Whitney U-test), further substantiating an upregulation of tau protein in neurons (Figure 2 p). These responses to SARS-CoV-2 infection did not yet lead to overt neurodegeneration, as quantified by counting NeuN-positive cells in the cortex ( $p > 0.05$ , t-test, Figure 2 e). Interestingly, the increase in hyper-phosphorylated tau or alpha-synuclein was not present in the dorsal hippocampus (cf. Figure 2 i, j, l), suggesting a regional specific vulnerability characteristic also to neurodegenerative diseases. Furthermore, we could observe a reduction of total Tau-positive cells in the hilar region of the dentate gyrus (Figure 2 k). Together with a trend to a reduction of NeuN-positive cells in this region ( $p > 0.05$ , t-test, Figure 2 m), this may indicate neuronal loss in specific subpopulations that requires further investigation. The lack of overt neurodegeneration is in line with absence of astrogliosis, quantified by analyzing astroglial cells and processes in cortex and hippocampus via area

covered by staining and qualitative assessment of cell morphology by an experienced researcher ( $p > 0.05$ , t-test, glial fibrillary acidic protein, GFAP-positive, data and staining not shown). Interestingly we observed subtle changes of GFAP-positive processes in the fimbriae hippocampi (white matter part of the dorsal hippocampus,  $p = 0.09$ , t-test, data and staining not shown), an observation which could be in line with communication of pathology along fiber tracts and previously suggested alterations of the blood brain barrier, thus requiring further attention.

## Discussion

In summary our results suggest localized microgliosis in the olfactory bulb in the absence of observable neuroinvasion in SARS-CoV-2 infected hamsters, and accumulation of hyper-phosphorylated tau and alpha-synuclein in cortical neurons. Latter observation is probably of significance to long lasting neurological symptoms in post-COVID-19 syndrome.

While virus can be identified in the CNS of infected hamsters 3 days post infection, only small amounts of virus are transiently present in the brain. As other groups could not identify viral proteins in the tissue,<sup>49</sup> our observations underline that, if any, only small amounts of SARS-CoV-2 enters the brain in the early phase of infection. Release of factors from local immune-cells or infected mucosa cells may provide a potential mechanism of communication between infected/inflamed nasal tissue and brain.<sup>54-55</sup> Similar observations of host response to combat viral entry were

evaluated area. **b-f.** suprahippocampal p-Tau-positive, Tau-positive, alpha-synuclein-positive and NeuN-positive cells, displayed as number (#) of cells per mm<sup>2</sup> of tissue. Note the differentiation in the stacked plots (b-d): the red color area are cells that have been counted as highly positive for the respective staining (cf. Material and methods), the white and gray parts of the bars are cell numbers of all other positively stained cells. Error bars display mean +/- SEM; n=10/group. **b.** p-Tau normally positive cells  $p = 0.46$  (Mann-Whitney U test (MWU)),  $p = 0.48$  (unpaired t-test (t-test)), highly positive cells  $p = 0.0015$  (MWU),  $p = 0.0006$  (t-test). Pooled cells (i.e. normally and highly positive cells)  $p = 0.0133$  (MWU),  $p = 0.164$  (t-test) **c.** Tau normally positive and highly positive cells, **d.** Alpha-synuclein normally and highly positive cells \* =  $p < 0.05$  (MWU or t-test). **e.** NeuN-positive cells, Dots represent the individual data values (N). **f.** Separate graph of p-Tau high cells from Figure 2 b with individual values. **g.** Receiver-operating characteristic (ROC) curves for p-Tau-positive cells. While normally p-Tau-positive cells do not perform well in the ROC curve (low AUC), highly p-Tau-positive cells are able to reliably differentiate between infected and mock animal (AUC 0.91,  $p = 0.0025$ ). **h.** Ratio between Tau-positive and NeuN-positive cells  $p = 0.03$  (MWU),  $p = 0.025$  (t-test) as mean +/- SEM and individual values (N). **i-m.** Evaluation of hippocampal p-Tau-positive, Tau-positive, alpha-synuclein-positive and NeuN-positive cells. **i.** Schematic drawing of the approximate position of the evaluated area: p-Tau-positive and alpha-synuclein-positive cells were counted in the whole hippocampal area (light green), Tau-positive and NeuN-positive cells were counted in the hilus of the dentate gyrus (dark green). **j-m.** hippocampal p-Tau-positive, Tau-positive, alpha-synuclein-positive and NeuN-positive cells, displayed as number (#) of cells per mm<sup>2</sup> of tissue, mean +/- SEM and individual values (N). **j.** p-Tau-positive cells  $p = 0.76$  (MWU),  $p = 0.79$  (t-test). **k.** Tau-positive cells  $p = 0.046$  (MWU),  $p = 0.046$  (t-test). **l.** alpha-synuclein-positive cells  $p = 0.3$  (MWU),  $p = 0.45$  (t-test). **m.** NeuN-positive cell  $p = 0.37$  (MWU),  $p = 0.21$  (t-test). **n-p.** Immunofluorescent images from suprahippocampal regions demonstrating stainings. Due to the tissue processing, residual blood is found in the blood vessels and remaining blood cells are unspecifically stained by binding of secondary antibodies (see white arrows for examples). **n.** NeuN-positive and p-Tau-positive staining in the suprahippocampal cortex comparing mock vs. SARS-CoV-2 infected tissue. White arrowheads point to exemplary cells stained for both NeuN (i.e. neurons) and p-Tau-positive cells. Scale bars: Overview 200  $\mu$ m, Close-up 50  $\mu$ m. **o.** Suprahippocampal cortical tissue of a SARS-CoV-2 infected hamster stained against NeuN and alpha-synuclein. The white arrowhead demonstrates a cell positive for alpha-synuclein and NeuN. Scale bars: Overview 200  $\mu$ m, Close-up 20  $\mu$ m. **p.** Tissue stained against NeuN and Tau in a SARS-CoV-2 infected animal. Hollow arrowheads point to exemplary cells expressing Tau and NeuN. White arrow heads point to a cell with a high amount of Tau staining. Scale bars: Overview 200  $\mu$ m, Close-up 20  $\mu$ m.

made for other viruses that enter via the olfactory system.<sup>56-58</sup> Therefore, it is important to compare our observations with other respiratory virus infections, such as influenza to enable identification of SARS-CoV-2 specific effects. These studies are underway in the influenza ferret model.

While this immune-response may build a local barrier of activated immune-cells in the brain to combat a potential arriving infection, its long term consequences on brain tissue could be harmful. Interestingly, a similar increase in tau pathology was recently demonstrated in 3D human brain organoids upon SARS-CoV-2 infection,<sup>59</sup> where infection led to a long-term mislocation of tau protein and an increase of phospho-tau accumulation in neuronal cells. In line with previous observations<sup>25,47</sup> we did not yet observe overt neurodegeneration at this time point after infection. In ongoing experiments we already confirmed persistence and further spreading of neuroinflammatory processes several weeks after infection, while further studies will characterize corresponding neuropathology and potential effects on cognitive function.

In autopsies of human COVID-19 patients the most common neurological findings were brain edema, cerebral infarcts and intracranial hemorrhages. In several cases histological evaluation revealed lymphocytic encephalitis and meningitis; many patients showed microglial activation and neuronophagy, such as intravascular microthrombi and hypoxic-ischemic injury. Fewer studies also describe neuronal cell loss, axon degeneration and alterations of blood vessels.<sup>13-20,60,61</sup> Interestingly, such autopsies also revealed that the microglial responses occurred regionally heterogeneous.<sup>21</sup> We argue that for most cases of post-COVID-19 syndrome one would not expect overt pathology in brain, mainly because additional contributing factors such as severe hypoxia, stroke, and overt systemic immune response are only expected for most severe cases. Additionally, we do not argue that COVID-19 results in acute and overt neurodegeneration, because there is no rapid increase in the number of patients with Parkinson's or Alzheimer's disease. However, these diseases have a long prodromal period and a risk phase where viral infections may act as triggers of pathological processes.

Further very recent studies corroborate our arguments. Analyses of brain lysates from COVID-19 patients revealed increased markers of inflammation and oxidative stress as well as activation of pathways causing tau hyper-phosphorylation typically associated with Alzheimer's disease, in the absence of virus in the brain.<sup>62</sup> Patients with neurological impairment due to COVID-19 showed significantly elevated plasma levels of t-tau, p-tau181, and other biomarkers relevant to Alzheimer's disease, correlating with the severity of COVID-19 and age.<sup>63</sup> Increased levels of such blood neuronal markers at admission are associated with death

due to COVID-19, with tau being the strongest predictor of mortality.<sup>64</sup> Patients with neurological symptoms persisting 1 to 3 months post COVID-19 infection showed increase of proteins related to neurodegenerative diseases (amyloid beta, neurofilament light chain, total tau, and p-tau181) in neuronal-enriched extracellular vesicle (nEV) pointing towards ongoing neurodegenerative processes.<sup>65</sup> Importantly, in a longitudinal imaging study comparing before and after infection, SARS-CoV-2 infection resulted in greater loss of gray matter compared to controls, especially in the orbitofrontal cortex and parahippocampal gyrus, increased markers of tissue damage in regions associated with taste and smell, and a greater reduction in overall brain size, even in mild to moderate cases. Patients post SARS-CoV-2 infection showed overall poorer performance in cognitive tests compared to the control group.<sup>66</sup>

In Parkinson's disease, alpha-synuclein pathology is thought to start in the olfactory bulb, the peripheral nervous system and the brain stem, thereby contributing to the diversity of motor and non-motor symptoms including cognitive, sleep, gastrointestinal and olfaction dysfunction as well as anxiety and depression in the prodromal phase.<sup>67</sup> Only specific neuronal subtypes, such as nigral dopaminergic neurons, degenerate overtly.<sup>68,69</sup> The overlap with post-COVID-19 symptoms is notable, and a significant subset of patients with Parkinson's disease presents with worsening of symptoms after remission of COVID-19.<sup>70</sup> Here we present evidence for a link between SARS-CoV-2 infection and the increase of molecular markers that also accumulate in neurodegenerative diseases. Whether this point towards initiation of neurodegenerative processes requires further studies on underlying pathogenic mechanisms, which rely on animal models, especially mouse models that give better access to genetic tools than the hamster. SARS-CoV-2 infected humanized ACE-2 (hACE2) mice show neuroinvasion and neuropathology,<sup>42</sup> which can be of advantage for proof of concept whether SARS-CoV-2 infection perpetuates proteinopathy. Alternatively, recent B1.351 and P1 variants may efficiently infect mice,<sup>[preprint study]<sup>71</sup></sup> and mouse-adapted viral strains have been developed<sup>72,73</sup>. Such viral strains could be used in in-depth characterized alpha-synuclein<sup>74,75</sup> or tau P301S<sup>76,77</sup> transgenic mice exposed to SARS-CoV-2 as 'second hit' strategy to unmask additive, synergistic or potentiating effects on pathology and neuronal function in a relatively short time period, as previously done with toxins/gene combinations.<sup>77</sup> Importantly, alpha-synuclein and tau represent key targets for disease-modifying therapy, such as reduction of expression, aggregation or spreading with antisense oligonucleotides, small molecules or specific antibodies, or the increase of protein degradation.<sup>79-83</sup> Given the increasing number of post-COVID-19 cases with symptoms resistant to treatment such studies are urgently required.

## Contributors

Conceptualization: CK, FR; Funding acquisition: FR, GG, WB; Supervision: FR, GG; Investigation: CK, CSS, ASH, ID; Animal experiments, necropsy, tissue processing and histological evaluation: SS, SB, TS, KB, GB, AB, WB, NM, BS; Statistical Analysis and visualization: CK, FR; Resources: GG, WB, AB; Manuscript preparation: CK, FR; AB, GB; Writing-Reviewing and editing: GG, WB, GB, AB, TS. CK, CSS and FR directly accessed and verified the underlying data reported in the manuscript. All authors read and approved the final version of the manuscript.

## Data Sharing Statement

Data supporting the figures of this manuscript are available from the corresponding author upon reasonable request.

## Declaration of interests

The authors declare that they have no conflict of interest.

## Acknowledgements

We thank Carolin Schütz and Julia Baskas for excellent technical assistance. Intramural funding was used for this study. The study was supported by a rapid response grant from the Federal Ministry of Health (BMG; ZMV I 1-2520COR501) to G.G. This study was supported by a BMBF (Federal Ministry of Education and Research) project entitled RAPID (Risk assessment in re-pandemic respiratory infectious diseases), 01KI1723G and by the Ministry of Science and Culture of Lower Saxony in Germany (14 - 76103-184 CORONA-15/20, and the EU SC1-PHE-CORONAVIRUS-2020 MANCO, no > 101003651). This study was in part supported by the Deutsche Forschungsgemeinschaft (DFG; German Research Foundation) -398066876/GRK 2485/1. TS was supported by the Luxemburgish National Research Fund (FNR, Project Reference: 15686728).

## Supplementary materials

Supplementary material associated with this article can be found in the online version at doi:10.1016/j.ebiom.2022.103999.

## References

- Helms J, Kremer S, Merdji H, Clere-Jehl R, Schenck M, Kummerlen C, et al. Neurologic features in severe SARS-CoV-2 infection. *N Engl J Med*. 2020.
- Mao L, Jin H, Wang M, Hu Y, Chen S, He Q, et al. Neurologic manifestations of hospitalized patients with coronavirus disease 2019 in Wuhan, China. *JAMA Neurol*. 2020.
- Varatharaj A, Thomas N, Ellul MA, Davies NWS, Pollak TA, Tenorio EL, et al. Neurological and neuropsychiatric complications of COVID-19 in 153 patients: a UK-wide surveillance study. *Lancet Psychiatry*. 2020;7(10):875–882.
- Ellul MA, Benjamin L, Singh B, Lant S, Michael BD, Easton A, et al. Neurological associations of COVID-19. *Lancet Neurol*. 2020;19(9):767–783.
- Heneka MT, Golenbock D, Latz E, Morgan D, Brown R. Immediate and long-term consequences of COVID-19 infections for the development of neurological disease. *Alzheimers Res Ther*. 2020;12(1):69.
- Taquet M, Geddes JR, Husain M, Luciano S, Harrison PJ. 6-month neurological and psychiatric outcomes in 236 379 survivors of COVID-19: a retrospective cohort study using electronic health records. *Lancet Psychiatry*. 2021;8(5):416–427.
- Ross Russell AL, Hardwick M, Jeyanantham A, White LM, Deb S, Burnside G, et al. Spectrum, risk factors and outcomes of neurological and psychiatric complications of COVID-19: a UK-wide cross-sectional surveillance study. *Brain Commun*. 2021;3(3):fcab168.
- Shah W, Hillman T, Playford ED, Hishmeh L. Managing the long term effects of covid-19: summary of NICE, SIGN, and RCGP rapid guideline. *BMJ*. 2021;372:n136.
- Lee MH, Perl DP, Nair G, Li W, Maric D, Murray H, et al. Microvascular injury in the brains of patients with COVID-19. *N Engl J Med*. 2021;384(5):481–483.
- Meinhardt J, Radke J, Dittmayer C, Franz J, Thomas C, Mothes R, et al. Olfactory transmucosal SARS-CoV-2 invasion as a port of central nervous system entry in individuals with COVID-19. *Nat Neurosci*. 2021;24(2):168–175.
- Puelles VG, Lutgehetmann M, Lindenmeyer MT, Sperhake JP, Wong MN, Allweiss L, et al. Multiorgan and renal tropism of SARS-CoV-2. *N Engl J Med*. 2020;383(6):590–592.
- Song E, Zhang C, Israelow B, Lu-Culligan A, Prado Alba V, Skriabine S, et al. Neuroinvasion of SARS-CoV-2 in human and mouse brain. Neuroinvasion of SARS-CoV-2 in humans and mice. *J Exp Med*. 2021;218(3).
- von Weyhern CH, Kaufmann I, Neff F, Kremer M. Early evidence of pronounced brain involvement in fatal COVID-19 outcomes. *Lancet*. 2020;395(10241):e109.
- Solomon IH, Normandin E, Bhattacharyya S, Mukerji SS, Keller K, Ali AS, et al. Neuropathological features of COVID-19. *N Engl J Med*. 2020;383(10):989–992.
- Matschke J, Lutgehetmann M, Hagel C, Sperhake JP, Schroder AS, Edler C, et al. Neuropathology of patients with COVID-19 in Germany: a post-mortem case series. *Lancet Neurol*. 2020;19(11):919–929.
- Kirschenbaum D, Imbach LL, Ulrich S, Rushing EJ, Keller E, Reimann RR, et al. Inflammatory olfactory neuropathy in two patients with COVID-19. *Lancet*. 2020;396(10245):166.
- Kirschenbaum D, Imbach LL, Rushing EJ, Frauenknecht KBM, Gascho D, Ineichen BV, et al. Intracerebral endothelitis and microbleeds are neuropathological features of COVID-19. *Neuropathol Appl Neurobiol*. 2021;47(3):454–459.
- Hernandez-Fernandez F, Sandoval Valencia H, Barbella-Aponte RA, Collado-Jimenez R, Ayo-Martin O, Barrena C, et al. Cerebrovascular disease in patients with COVID-19: neuroimaging, histological and clinical description. *Brain*. 2020;143(10):3089–3103.
- Deigendesch N, Sironi L, Kutza M, Wischniewski S, Fuchs V, Hench J, et al. Correlates of critical illness-related encephalopathy predominate postmortem COVID-19 neuropathology. *Acta Neuropathol*. 2020;140(4):583–586.
- Al-Dalahmah O, Thakur KT, Nordvig AS, Prust ML, Roth W, Lignelli A, et al. Neuronophagia and microglial nodules in a SARS-CoV-2 patient with cerebellar hemorrhage. *Acta Neuropathol Commun*. 2020;8(1):147.
- Thakur KT, Miller EH, Glendinning MD, Al-Dalahmah O, Banu MA, Boehme AK, et al. COVID-19 neuropathology at Columbia university irving medical center/New York Presbyterian Hospital. *Brain*. 2021;144(9):2696–2708.
- Schwabenland M, Salie H, Tanevski J, Killmer S, Lago MS, Schlaak AE, et al. Deep spatial profiling of human COVID-19 brains reveals neuroinflammation with distinct microanatomical microglia-T-cell interactions. *Immunity*. 2021.
- Blank T, Detje CN, Spiess A, Hagemeyer N, Brendecke SM, Wolfart J, et al. Brain endothelial- and epithelial-specific interferon receptor chain 1 drives virus-induced sickness behavior and cognitive impairment. *Immunity*. 2016;44(4):901–912.
- Chhatbar C, Detje CN, Grabski E, Borst K, Spanier J, Ghita L, et al. Type I interferon receptor signaling of neurons and astrocytes reg-

- ulates microglia activation during viral encephalitis. *Cell Rep.* 2018;25(1):118–129. e4.
- 25 Zhang L, Zhou L, Bao L, Liu J, Zhu H, Lv Q, et al. SARS-CoV-2 crosses the blood-brain barrier accompanied with basement membrane disruption without tight junctions alteration. *Signal Transduct Target Ther.* 2021;6(1):337.
- 26 Seessle J, Waterboer T, Hippchen T, Simon J, Kirchner M, Lim A, et al. Persistent symptoms in adult patients one year after COVID-19: a prospective cohort study. *Clin Infect Dis.* 2021.
- 27 Hosp Jonas A, Dressing A, Blazhenets G, Bormann T, Rau A, Schwabenland M, et al. Cognitive impairment and altered cerebral glucose metabolism in the subacute stage of COVID-19. *Brain A J Neurol.* 2021;144(4):1263–1276.
- 28 Blomberg B, Mohn KG, Brokstad KA, Zhou F, Linchausen DW, Hansen BA, et al. Long COVID in a prospective cohort of home-isolated patients. *Nature Med.* 2021.
- 29 Wildburger NC, Hartke AS, Schidlitzki A, Richter F. Current evidence for a bidirectional loop between the lysosome and alpha-synuclein proteoforms. *Front Cell Dev Biol.* 2020;8:598446.
- 30 Chakroun T, Evsyukov V, Nykanen NP, Hollerhage M, Schmidt A, Kamp F, et al. Alpha-synuclein fragments trigger distinct aggregation pathways. *Cell Death Dis.* 2020;11(2):84.
- 31 Kovacs GG, Lukic MJ, Irwin DJ, Arzberger T, Respondek G, Lee EB, et al. Distribution patterns of Tau pathology in progressive supranuclear palsy. *Acta Neuropathol.* 2020;140(2):99–119.
- 32 Richter F. Alpha-synuclein as therapeutic target in Parkinson's disease. *Neuroforum.* 2019;25(2).
- 33 Hoglinger GU, Alvarez-Fischer D, Arias-Carrion O, Djufri M, Windolph A, Keber U, et al. A new dopaminergic nigro-olfactory projection. *Acta Neuropathol.* 2015;130(3):333–348.
- 34 Sampson TR, Debelius JW, Thron T, Janssen S, Shastri GG, Ilhan ZE, et al. Gut microbiota regulate motor deficits and neuroinflammation in a model of Parkinson's disease. *Cell.* 2016;167(6):1469–1480. e12.
- 35 Vasili E, Dominguez-Mejide A, Outeiro TF. Spreading of alpha-synuclein and Tau: a systematic comparison of the mechanisms involved. *Front Mol Neurosci.* 2019;12:107.
- 36 Uemura N, Ueda J, Yoshihara T, Ikuno M, Uemura MT, Yamakado H, et al. Alpha-synuclein spread from olfactory bulb causes hypomania, anxiety, and memory loss in BAC-SNCA mice. *Mov Disord.* 2021;36(9):2036–2047.
- 37 Zickler M, Stanelle-Bertram S, Ehret S, Heinrich F, Lange P, Schaumburg B, et al. Replication of SARS-CoV-2 in adipose tissue determines organ and systemic lipid metabolism in hamsters and humans. *Cell Metab.* 2022;34(1):1–2.
- 38 Becker K, Beythien G, de Buhr Nicole SBS, et al. Vasculitis and neutrophil extracellular traps in lungs of golden Syrian hamsters with SARS-CoV-2. *Front Immunol.* 2021;12:640842.
- 39 Allnoch L, Beythien G, Leitzen E, Becker K, Kaup FJ, Stanelle-Bertram S, et al. Vascular inflammation is associated with loss of aquaporin 1 expression on endothelial cells and increased fluid leakage in SARS-CoV-2 infected golden Syrian hamsters. *Viruses.* 2021;13(4).
- 40 Käufer C, Chhatbar C, Bröer S, et al. Chemokine receptors CCR2 and CX3CR1 regulate viral encephalitis-induced hippocampal damage but not seizures. *Proc Natl Acad Sci U S A.* 2018;115(38):E8929–E8938. <https://doi.org/10.1073/pnas.1806754115>. Epub 2018 Sep 4. PMID: 30181265; PMCID: PMC6156634.
- 41 Schindelin J, Arganda-Carreras I, Frise E, Kaynig V, Longair M, Pietzsch T, et al. Fiji: an open-source platform for biological-image analysis. *Nat Methods.* 2012;9(7):676–682.
- 42 Lee CY, Lowen AC. Animal models for SARS-CoV-2. *Curr Opin Virol.* 2021;48:73–81.
- 43 Chan JF, Zhang AJ, Yuan S, Poon VK, Chan CC, Lee AC, et al. Simulation of the clinical and pathological manifestations of coronavirus disease 2019 (COVID-19) in a golden Syrian hamster model: implications for disease pathogenesis and transmissibility. *Clin Infect Dis.* 2020;71(9):2428–2446.
- 44 Kim T, Lee JS, Ju YS. Experimental models for SARS-CoV-2 infection. *Mol Cells.* 2021;44(6):377–383.
- 45 Shou S, Liu M, Yang Y, Kang N, Song Y, Tan D, et al. Animal models for COVID-19: hamsters, mouse, ferret, mink, tree shrew, and non-human primates. *Front Microbiol.* 2021;12:626553.
- 46 Alipoor Shamila D, Mortaz E, Varahram M, Garssen J, Adcock Ian M. The immunopathogenesis of neuroinvasive lesions of SARS-CoV-2 infection in COVID-19 patients. *Front Neurol.* 2021;12:1300.
- 47 de Melo GD, Lazarini F, Levallois S, Hautefort C, Michel V, Larrous F, et al. COVID-19-related anosmia is associated with viral persistence and inflammation in human olfactory epithelium and brain infection in hamsters. *Sci Transl Med.* 2021;13(596).
- 48 de Melo GD, Lazarini F, Larrous F, Feige L, Kornobis E, Levallois S, et al. Attenuation of clinical and immunological outcomes during SARS-CoV-2 infection by ivermectin. *EMBO Mol Med.* 2021;13(8):e14122.
- 49 Bryche B, St Albin A, Murri S, Lacote S, Pulido C, Ar Guillou M, et al. Massive transient damage of the olfactory epithelium associated with infection of sustentacular cells by SARS-CoV-2 in golden Syrian hamsters. *Brain Behav Immun.* 2020;89:579–586.
- 50 Furube E, Kawai S, Inagaki H, Takagi S, Miyata S. Brain region-dependent heterogeneity and dose-dependent difference in transient microglia population increase during lipopolysaccharide-induced inflammation. *Sci Rep.* 2018;8(1):2203.
- 51 Hasegawa-Ishii S, Imamura F, Nagayama S, Murata M, Shimada A. Differential effects of nasal inflammation and odor deprivation on layer-specific degeneration of the mouse olfactory bulb. *Eneuro.* 2020;7(2).
- 52 Hasegawa-Ishii S, Shimada A, Imamura F. Lipopolysaccharide-initiated persistent rhinitis causes gliosis and synaptic loss in the olfactory bulb. *Sci Rep.* 2017;7: Uk.
- 53 Salimi M, Ghazvineh S, Zare M, Parsazadegan T, Dehdar K, Nazari M, et al. Distraction of olfactory bulb-medial prefrontal cortex circuit may induce anxiety-like behavior in allergic rhinitis. *Plos One.* 2019;14(9).
- 54 Moseman EA, Blanchard AC, Nayak D, McGavern DB. T cell engagement of cross-presenting microglia protects the brain from a nasal virus infection. *Sci Immunol.* 2020;5(48).
- 55 Durrant DM, Ghosh S, Klein RS. The olfactory bulb: an immunosensory effector organ during neurotropic viral infections. *ACS Chem Neurosci.* 2016;7(4):464–469.
- 56 Detje CN, Lienenklaus S, Chhatbar C, Spanier J, Prajeeth CK, Soldner C, et al. Upon intranasal vesicular stomatitis virus infection, astrocytes in the olfactory bulb are important interferon Beta producers that protect from lethal encephalitis. *J Virol.* 2015;89(5):2731–2738.
- 57 Detje CN, Meyer T, Schmidt H, Kreuz D, Rose JK, Bechmann I, et al. Local type I IFN receptor signaling protects against virus spread within the central nervous system. *J Immunol.* 2009;182(4):2297–2304.
- 58 Kalinke U, Bechmann I, Detje CN. Host strategies against virus entry via the olfactory system. *Virulence.* 2011;2(4):367–370.
- 59 Ramani A, Muller L, Ostermann PN, Gabriel E, Abida-Islam P, Muller-Schiffmann A, et al. SARS-CoV-2 targets neurons of 3D human brain organoids. *EMBO J.* 2020;39(20):e106230.
- 60 Fabbri VP, Foschini MP, Lazzarotto T, Gabrielli L, Cenacchi G, Gallo C, et al. Brain ischemic injury in COVID-19-infected patients: a series of 10 post-mortem cases. *Brain Pathol.* 2021;31(1):205–210.
- 61 Bryce C, Grimes Z, Pujadas E, Ahuja S, Beasley MB, Albrecht R, et al. Pathophysiology of SARS-CoV-2: the Mount Sinai COVID-19 autopsy experience. *Mod Pathol.* 2021;34(8):1456–1467.
- 62 Reiken S, Sittenfeld L, Dridi H, Liu Y, Liu X, Marks AR. Alzheimer's-like signaling in brains of COVID-19 patients. *Alzheimers Dement.* 2022.
- 63 Frontera JA, Boutajangout A, Masurkar AV, Betensky RA, Ge Y, Vedvyas A, et al. Comparison of serum neurodegenerative biomarkers among hospitalized COVID-19 patients versus non-COVID subjects with normal cognition, mild cognitive impairment, or Alzheimer's dementia. *Alzheimers Dement.* 2022.
- 64 De Lorenzo R, Loré NI, Finardi A, Mandelli A, Cirillo DM, Tresoldi C, et al. Blood neurofilament light chain and total Tau levels at admission predict death in COVID-19 patients. *J Neurol.* 2021;268(12):4436–4442.
- 65 Sun B, Tang N, Peluso MJ, Iyer NS, Torres L, Donatelli JL, et al. Characterization and biomarker analyses of post-COVID-19 complications and neurological manifestations. *Cells.* 2021;10(2).
- 66 Douaud G, Lee S, Alfaro-Almagro F, Arthofer C, Wang C, McCarthy P, et al. SARS-CoV-2 is associated with changes in brain structure in UK Biobank. *Nature.* 2022.
- 67 Berg D, Borghammer P, Fereshthehnejad SM, Heinzel S, Horsager J, Schaeffer E, et al. Prodromal Parkinson disease subtypes - key to understanding heterogeneity. *Nat Rev Neurol.* 2021;17(6):349–361.
- 68 Hirsch E, Graybiel AM, Agid YA. Melanized dopaminergic neurons are differentially susceptible to degeneration in Parkinson's disease. *Nature.* 1988;334(6180):345–348.
- 69 Del Tredici K, Braak H. Lewy pathology and neurodegeneration in premotor Parkinson's disease. *Mov Disord.* 2012;27(5):597–607.

- 70 Leta V, Rodriguez-Violante M, Abundes A, Rukavina K, Teo JT, Falup-Pecurariu C, et al. Parkinson's disease and post-COVID-19 syndrome: the Parkinson's long-COVID spectrum. *Mov Disord*. 2021;36(6):1287–1289.
- 71 Montagutelli X, Prot M, Levillayer L, Salazar Eduard B, Jouvion G, Conquet L, et al. The B1.351 and P.1 variants extend SARS-CoV-2 host range to mice. *bioRxiv*. 2021. <https://doi.org/10.1101/2021.03.18.436013>.
- 72 Leist SR, Dinnon KH, Schafer A, Tse LV, Okuda K, Hou YJ, et al. A mouse-adapted SARS-CoV-2 induces acute lung injury and mortality in standard laboratory mice. *Cell*. 2020;183(4):1070–1085. e12.
- 73 Dinnon KH, Leist SR, Schafer A, Edwards CE, Martinez DR, Montgomery SA, et al. A mouse-adapted model of SARS-CoV-2 to test COVID-19 countermeasures. *Nature*. 2020;586(7830):560–566.
- 74 Chesselet MF, Richter F, Zhu C, Magen I, Watson MB, Subramaniam SR. A progressive mouse model of Parkinson's disease: the Thy1-aSyn ("Line 61") mice. *Neurotherapeutics*. 2012;9(2):297–314.
- 75 Chesselet MF, Richter F. Modelling of Parkinson's disease in mice. *Lancet Neurol*. 2011;10(12):1108–1118.
- 76 Allen B, Ingram E, Takao M, Smith MJ, Jakes R, Virdee K, et al. Abundant Tau filaments and nonapoptotic neurodegeneration in transgenic mice expressing human P301S Tau protein. *J Neurosci*. 2002;22(21):9340–9351.
- 77 Hollerhage M, Deck R, De Andrade A, Respondek G, Xu H, Rosler TW, et al. Piericidin A aggravates Tau pathology in P301S transgenic mice. *PLoS One*. 2014;9(12):e13557.
- 78 Richter F, Gabby L, McDowell KA, Mulligan CK, De L, Rosa K, Sioshansi PC, et al. Effects of decreased dopamine transporter levels on nigrostriatal neurons and paraquat/maneb toxicity in mice. *Neurobiol Aging*. 2017;51:54–66.
- 79 Richter F, Subramaniam SR, Magen I, Lee P, Hayes J, Attar A, et al. A molecular tweezer ameliorates motor deficits in mice overexpressing alpha-synuclein. *Neurotherapeutics*. 2017;14(4):1107–1119.
- 80 Helmschrodt C, Höbel S, Schöniger S, Bauer A, Bonicelli J, Gringmuth M, et al. Polyethylenimine nanoparticle-mediated siRNA delivery to reduce  $\alpha$ -synuclein expression in a model of Parkinson's disease. *Mol Ther Nucl Acids*. 2017;9:57–68.
- 81 Richter F, Fleming SM, Watson M, Lemesre V, Pellegrino L, Ranes B, et al. A G case chaperone improves motor function in a mouse model of synucleinopathy. *Neurotherapeutics*. 2014;11(4):840–856.
- 82 Magen I, Ostritsky R, Richter F, Zhu C, Fleming SM, Lemesre V, et al. Intranasal NAP (davunetide) decreases Tau hyperphosphorylation and moderately improves behavioral deficits in mice overexpressing alpha-synuclein. *Pharmacol Res Perspect*. 2014;2(5):e00065.
- 83 Rosler TW, Costa M, Hoglinger GU. Disease-modifying strategies in primary Tauopathies. *Neuropharmacology*. 2020;167:107842.